

# Multi-sensor method of producing a material independent inductive distance measuring device

S. Johnstone

*School of Engineering, University of Durham, UK*

## Abstract

In harsh industrial applications, it is often necessary to measure the distance between metal objects, e.g. to determine the shape of a steel strip. Due to the presence of hot steam, water and dirt, inductive sensors are typically used but they have to be recalibrated each time the target material is replaced or the sensor is moved laterally. This work investigates the use of the sensor system to reduce the effects of material property variations. This design also enables a lateral movement compensation algorithm to be applied, thus leading the way to a true target independent distance-measuring device.

This paper investigates a novel method of compensating for the effects of material property variations on distance measurement using a sensor consisting of a permanent magnet and a 500 kHz eddy current device. This was achieved by producing empirical models for each of the sensor outputs. Results on steel samples transforming from the austenite to ferrite phase show that, for slow changing material variations of less than 3Hz, the error in the distance measurement can be reduced from 37% to less than 2%.

*Keywords: inductive sensors, distance measurement, non-destructive testing.*

## 1 Introduction

In harsh industrial environments such as steel mills, metal component fabrication plants etc it is often desirable to measure the dimensions of products and or actuators of machinery used in the process. Examples include measuring the profile of steel strip at speeds up to  $12\text{ms}^{-1}$  or locating an actuator controlling the size of a mould used for casting steel products. Because the product is often at high temperature in these processes there are several factors which can affect the



integrity of a distance measurement. Firstly, there is the presence of steam and dust which excludes the use of direct line of sight optical techniques such as laser Doppler and time-of flight techniques [1]. Variation in the humidity would affect the accuracy of ultrasonic and capacitance methods. Thus, inductive methods were considered as a possible solution to this measurement problem. Inductive sensors are readily available to buy [2], but need to be calibrated to the target material and they are particularly sensitive to whether the material is ferromagnetic. This problem was addressed by Bruel and Kjar <sup>TM</sup>[3] by making use of electrical phase information, but the sensor was too difficult to manufacture and was withdrawn from the market. Placko *et al.* [4] have reported a sensor which can measure the thickness of the coating on galvanised steel strip at temperatures around 40°C and 300°C using a differential method together with an analytical small perturbation complex reluctance model. There has also been work reported on compensating for lift-off variations whilst measuring the material properties of steel [5,6]. Yin *et al.* [7] describe a simple model to simultaneously measure the thickness and distance of non-magnetic metals.

This paper investigates using a combined dc magnetic and eddy current sensor system to compensate for the material variations of steel, as it cools from a paramagnetic to a ferromagnetic state, to give a material independent distance measuring device. The general measurement principle is described followed by investigations into the design of a prototype. Using these results, a material compensation algorithm is presented, together with the results of its application.

## 2 General measurement principle

The general measurement principle is to apply a magnetic field around the target of interest. Figure 1 shows two possible geometries in which the magnetic field can be either ac or dc. The strength of the magnetic flux density measured at one of the poles is dependent on the distance of the sensor from the target, the target size and material. If, for example the target: sensor diameter ratio is large and the material property constant, then the relationship between the  $\underline{B}$ -field and sensor: target distance,  $x$ , (lift-off) along the centreline of a pole radius,  $a$ , can be given by eqn (1)

$$\underline{B} = \frac{k}{(a^2 + x^2)^{3/2}} \quad (1)$$

where  $k$  is a constant. For the case of  $x < a$ , this can be approximated to

$$\underline{B} = \frac{k'}{1 + \frac{3}{2} \left( \frac{x}{a} \right)^2} \quad (2)$$

where  $k' = k/a^3$ .



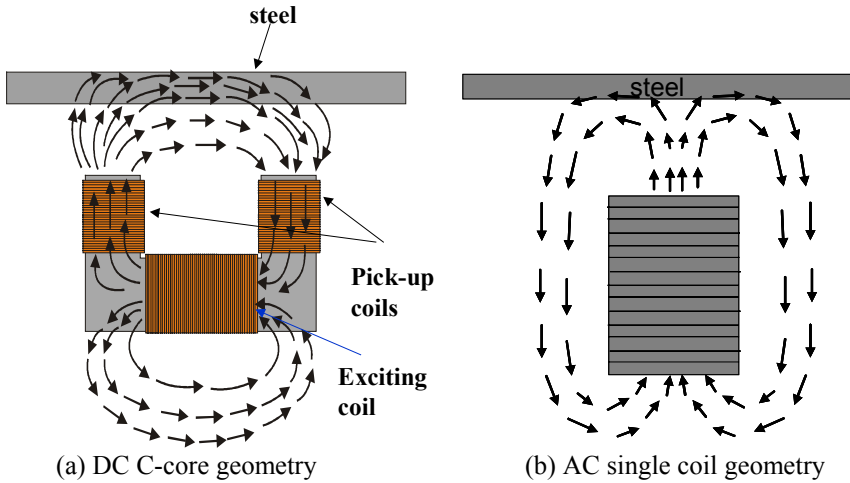


Figure 1: Sensor geometries.

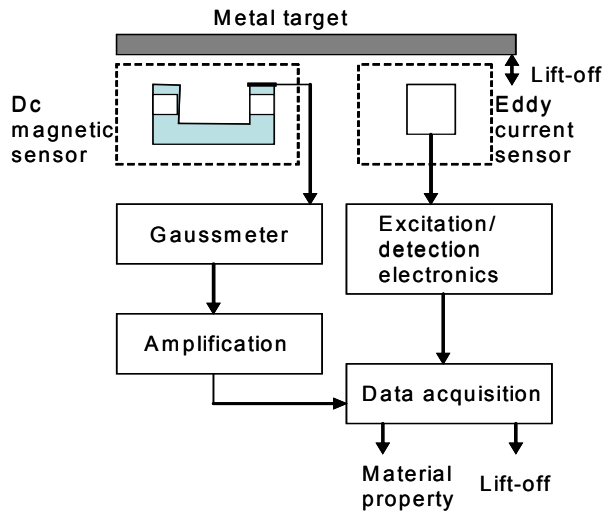


Figure 2: Sensor system.

For dc systems a sensor is required to measure the magnetic flux density and for ac systems the change in coil impedance is used.

### 3 Experimentation

The system investigated consisted of a dc C-core permanent magnet with a Hall probe and a Kaman 10CU eddy current sensor as shown in Figure 2.

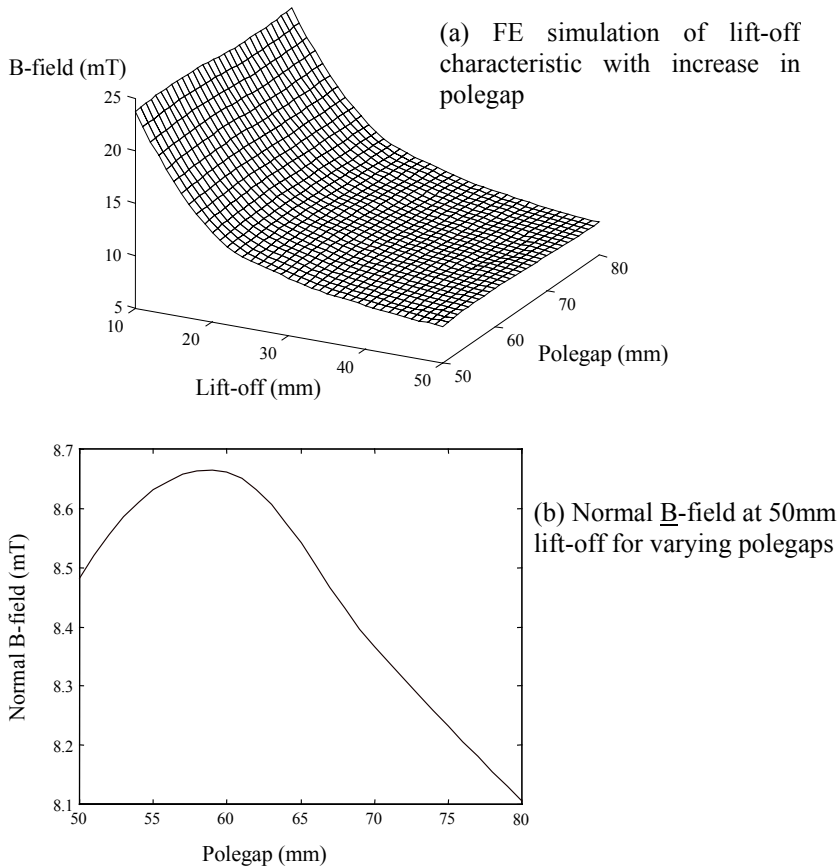


Figure 3: FE simulations showing the relationship between B-Field and lift-off and polegap.

For the C-core, an Alcomax III magnet was chosen due to its high remanance of 1.26T and low reversible temperature coefficient of  $-0.02\ \% / ^\circ\text{C}$ . A C-core geometry was used to increase the volume of the magnet and thus the magnetic flux density in the air gap as shown in eqn (3).

$$B_{\text{gap}} H_{\text{gap}} \tau_{\text{gap}} = -B_{\text{magnet}} H_{\text{magnet}} \tau_{\text{magnet}}, \quad (3)$$

Finite element simulations using Ansoft Maxwell<sup>TM</sup> were used to determine the optimum polegap: lift-off ratio. Figure 3(a) shows the relationship between the normal component  $\underline{B}$ -field and the two variables; lift-off and polegap. Figure 3(b) shows the effect the polegap has at a lift-off of 50mm. It shows that the optimum sensitivity to lift-off occurs when the polegap: lift-off ratio is slightly greater than one. This is because for smaller polegaps, the flux will preferentially travel directly between the poles and for larger ratios it is more sensitive to the material property.

The next major component in the system was a commercial inductive sensor, the Kaman 10CU. It was quoted as having a linear measurement range of 50mm. Figure 4 shows the output for a range of materials. It shows that for this sensor, it is more sensitive to material property variations at lower lift-offs.

Two sensors were used in this instrument such that the material properties of the target material and the lift-off could be decoupled. Thus, the sensors were required to be as close together as possible without interfering with each other such that they were measuring the same part of the target. The arrangement which resulted in the smallest footprint is shown in Figure 2.

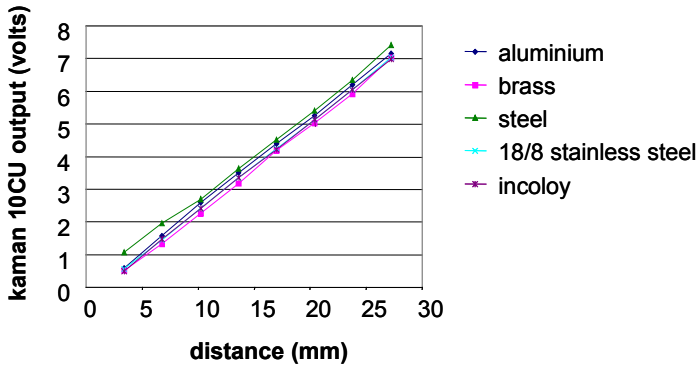


Figure 4: Lift-off characteristics for the Kaman 10CU probe.

In the experiments the target materials were designed to have diameters of at least three times that of the sensor system footprint and thicknesses of at least 100 times the skin depth such that the system was relatively insensitive to any variations in the target material dimensions.

#### 4 Speed and temperature compensation

When using this sensor to measure lift-off, there will often be motion between the sensor and the target. Tests were carried out to assess the effect of this motion together with the orientation of the C-core dc system. The results for the dc sensor system show that the dc system is least sensitive to motion when the field is perpendicular to the direction of motion. The detailed mechanism behind was not investigated in this study.

To assess the temperature characteristic, the system was placed in an environmental chamber. Due to the large thermal inertia of the magnet, a settling time of 4 hours was used. The temperature was measured using a resistive temperature device. First order models for this and the eddy current sensor were found to be

$$V_{dc} = V_{measured,dc} + 1.38 \times (V_{RTD} - 2.00) \quad (4)$$

$$V_{\text{eddy}} = V_{\text{measured,Eddy}} + 0.431 \times (V_{\text{RTD}} - 2.00) \quad (5)$$

where  $V_{\text{dc}}$  and  $V_{\text{eddy}}$  are the temperature corrected voltages for the dc and eddy current sensors respectively.

## 5 Material compensation algorithm

This consisted of developing an analytical model for each of the two sensing components when a single material property, the magnetic permeability, changed. It was assumed that there was no interaction between the two sensors.

### 5.1 DC magnetic sensor model

Experiments show that the sensor output can be represented as being proportional to the magnetic property of the target,  $M(F)$ , where  $F$  is the fraction of ferromagnetic material and  $1-F$  is the fraction of paramagnetic material in the target. The Biot-Savart law suggests that for lift-off: pole diameter ratios less than unity, the output has a form similar to  $1/x^2$ . With no sample present, the Hall probe gives an output,  $V_b$ . Hence,

$$V_{\text{dc}} = V_b + \frac{k_{\text{dc}} M(F)}{x^2}, \quad (6)$$

where  $k_{\text{dc}}$  is a constant.

### 5.2 Eddy current sensor model

For a given material, the eddy current sensor is set up with the manufacturer's calibration equation. Using experimental data, the output,  $V_{\text{eddy}}$  is also shown to be proportional to the target's change in magnetic property,  $P(F)$ , the effect of which decreases with distance, again following an inverse square law.

$$V_{\text{eddy}} = \frac{x}{4} - 2.5 + \frac{k_{\text{eddy}} P(F)}{x^2}, \quad (7)$$

where  $k_{\text{eddy}}$  is a constant.

One point to note, is that the dc sensor measures all the way through the sample, whereas the eddy current sensor looks through a thin layer whose thickness is determined by the skin depth,  $\delta$ , which decreases as the sample transforms and becomes more magnetic.

### 5.3 Estimation of constants

To simplify the model, the magnetic property was assumed to be directly proportional to the fraction of ferromagnetic material, i.e.



$$k_{dc} \cdot M(F) = k_d \cdot F. \quad (8)$$

The sensor system was placed at known distances below a heated steel sample and the outputs recorded for both the dc and ac sensors. A temperature sensor was used to identify the region at which the steel transformed to the ferromagnetic phase. It was assumed that the sensor output before the transformation point corresponded to 0% ferromagnetic fraction and the room temperature output, 100%. Typical traces are shown in Figure 5. It can be seen that the dc sensor behaves in the same manner as described by the model. However, the eddy current sensor shows a rise in output during the transformation process but then reduces after. Thus, this model was restricted to the transformation region where the predominant change has been found to be [8] the magnetic properties. The reason for the decrease is considered to be due to a change in conductivity due to temperature and microstructure. Thus, the direct relationship with a material property is more complex to extract in the post transformation region.

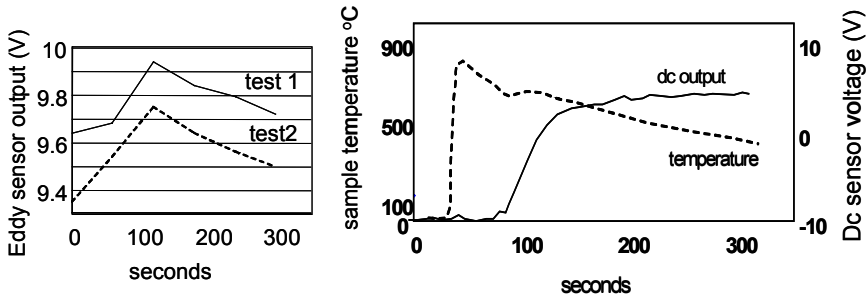


Figure 5: Output of eddy current and dc sensors for a steel target transforming from the paramagnetic to ferromagnetic state.

By applying the constants for eqns (6) and (7) and rearranging the following two relationships were found

$$F = \frac{(V_{dc} + 8.81)}{1130} \cdot \left[ V_{eddy} + 2.50 - \frac{(V_{dc} + 8.81)}{34.0} \right]^2 \quad (9)$$

$$x = \sqrt{\frac{18100 \cdot F}{V_{dc} + 8.81}} \quad (10)$$

## 6 Hot tests

The sensor system was then placed under water cooled steel strip which had been heated in a furnace and passed over the sensor. Figures 6 and 7 show the signals

from the dc sensor and eddy current sensor before and after the application of the material compensation algorithm for a brittle grade of steel.

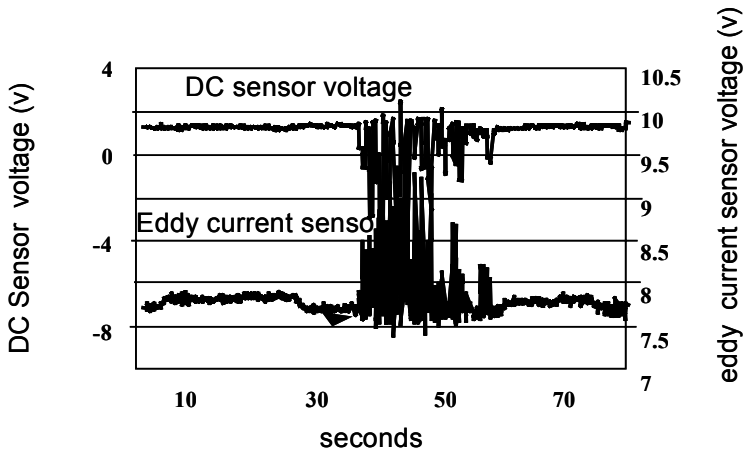


Figure 6: Temperature compensated signals recorded using the sensor system for a brittle grade of steel.

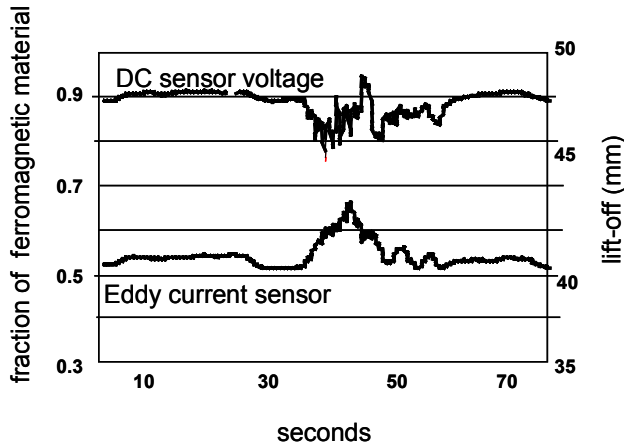


Figure 7: Calculated ferromagnetic content and lift-off for a steel sample.

Figure 6 shows a region of measurements in which there was a variation on the eddy current sensor output equivalent to 37% of the signal range, with a corresponding disturbance in the dc sensor output. After the algorithm was applied, this was reduced to a residual variation of about 2% as shown in Figure 7. This was confirmed by the fact that the Hall probe trace is depressed in the same region as the eddy current sensor output increases.

## 7 Discussion

The magnetic field from a dc system will penetrate fully through the sample, and thus is strongly affected by the average material property. Commercial lift-off

sensors use much higher frequencies such as 500kHz to minimise the depth of penetration, characterised by the skin depth, and hence the effect of the material; thus giving a higher accuracy measurement. The results presented in this paper show that these two effects combine to reduce errors due to material properties. There still remains a residual error of around 2%, however. Possible factors and their effects are discussed below.

- i) The target steel being below the transformation temperature, since it varies with cooling rate and variations in chemical composition. The model for the eddy current sensor does not apply in this region as shown in Figure 5.
- ii) First order models have been used to derive the temperature characteristic and the sensor outputs. Thus, higher order effects have been ignored.
- iii) The two sensor outputs have considerably different bandwidths which affects their response times. A mismatch of sample times could act to amplify the disturbance.
- iv) The sensors, although close together are not sampling exactly the same target area.

## 8 Conclusions

A prototype dual sensor system has been designed and constructed to measure the distance to metallic targets. It consists of a dc C-core and a commercial eddy current sensor.

Algorithms have been developed and applied to measure the distance to metallic target materials (lift-off) without being affected by variations in the material properties and temperature.

Hot tests have been used to vary the ferromagnetic properties of the target whilst measuring the lift-off. The algorithms have been shown to reduce the errors due to material property variation from 37% to 2%.

Factors contributing to the final 2% error have been identified as

- a. the non-linearity of the eddy current output outside the transformation region,
- b. the neglect of higher order effects,
- c. the different bandwidths of the sensors and
- d. the sensors seeing different target areas.

## Acknowledgements

The author wishes to thank Professor A Peyton and Dr WDN Pritchard for their guidance.

## References

- [1] Webster, J.G, The measurement , instrumentation and sensors handbook (The electrical engineering handbook series), IEEE Press, 1999.
- [2] Kaman Products, <http://www.kamansensors.com/html/core.htm>, 2004



- [3] Bruel and Kjar, New Product Flyer, 2000.
- [4] Placko, D., Clergeot, H.& Santander, E., Physical modelling of an eddy current sensor designed for real time distance and thickness measurement in galvanisation industry. *IEEE Transactions on Magnetics*, **25(4)**, pp. 1989.
- [5] Johnstone, S., Binns, R., Peyton, A.J. & Pritchard, W.D.N., Using electromagnetic methods to monitor the transformation of steel samples, *Transactions of the Institute of Measurement and Control*, **23(1)**, pp. 21-29, 2001.
- [6] Yasuhiro, M. & Seigo, A., Transformation rate-measuring method and device, NKK Corporation, Pub No 07191991, August 1995.
- [7] Yin, W.L., Peyton, A.J., Dickinson, S.J., Simultaneous measurement of distance and thickness of a thin metal plate with an electromagnetic sensor using a simplified model, *IEEE Transactions on Instrumentation and Measurement*, **53 (4)**, pp. 1335-1338, 2004.
- [8] Bozorth, R.M., *Ferromagnetism*, Bell Laboratory Series 1964.

